Biochimica et Biophysica Acta, 1100 (1992) 67–74

BbABIO 43590

Determination of the position of the $Q_i^{\cdot-}$ quinone binding site from the protein surface of the cytochrome bc_1 complex in *Rhodobacter capsulates* chromatophores

Steven W. Meinhardt [a] and Tomoko Ohnishi [b]

[a] *Department of Biochemistry, North Dakota State University, Fargo, ND and* [b] *Department of Biochemistry and Biophysics, University of Pennsylvania, Philadelphia, PA (USA)*

(Received 10 September 1991)
(Revised manuscript received 10 January 1992)

Key words: Cytochrome bc_1 complex; EPR; Semiquinone anion site; (*Rb. capsulatus*)

The technique of distance measurement utilizing spin relaxation enhancement by an external probe, has been extended to the study of intrinsic semiquinone radicals through the use of holmium-EDTA complexes and continuous wave electron paramagnetic resonance spectroscopy. This technique has been used to determine the distance of the semiquinone anion, Q_i (also designated as $Q_n^{\cdot-}$ or $Q_c^{\cdot-}$), from the surface of the ubiquinone cytochrome *c* oxidoreductase, consisting of only three subunits, in membrane particles from *Rhodobacter capsulates*. The location of the semiquinone anion is 6–10 Å from the N side protein, establishing that there are two separate quinone reaction sites, i.e., 'Q_i' and 'Q_o', within this complex on opposite sides of the membrane. The results are discussed in relation to reported ENDOR, EPR, and optical studies of the mitochondrial counterpart.

Introduction

The ubiquinol cytochrome *c* oxidoreductase (also designated as the cytochrome bc_1 complex, or complex III) is the most thoroughly characterized of the mitochondrial electron transport complexes. The protein subunit [1–3] and prosthetic group composition [4–6], number and types of inhibitor reaction sites [7,8], as well as the physicochemical properties of the prosthetic groups [9–13], have been studied. The Q cycle, first proposed by P. Mitchell [14] and later modified by others [15,16], provides a detailed model which explains roles of all prosthetic groups, sites of action of the inhibitors, as well as the mechanism of the coupling of electron transport to proton translocation. An essential feature of this model is the presence of two separate quinone reaction sites in equilibrium with the aqueous phase on opposite sides of the membrane. The reactions of the ubiquinone oxidation site, the 'Q_o' site (also named as 'Q_p' or 'Q_z' site) are inhibited by compounds such as myxothiazol [17–19], UHDBT [20,21], and stigmatellin [22,23]. This site is formed by the cytochrome *b* protein in close association with the Rieske iron-sulfur protein. The Q_o site does not thermodynamically stabilize a ubisemiquinone species, although ubisemiquinone signals at this site can be observed under turnover conditions in the presence of antimycin [24]. The site for the reduction of ubiquinone has been shown to contain a thermodynamically stable ubisemiquinone species, $Q_i^{\cdot-}$ (also named $Q_n^{\cdot-}$ or $Q_c^{\cdot-}$) whose physicochemical properties have been described in the mitochondrial complex [25–29], the cytochrome bc_1 complex in *Paraccocus denitrificans* [30], as well as in the photosynthetic bacteria, *Rhodobacter capsulatus* [31] and *Rhodobacter spheroides* [32,33]. This semiquinone species is in the anion form [27,29,31] in the physiological pH range and is completely destabilized by the inhibitor, antimycin [27,29].

Several groups have investigated the positions of the redox centers relative to the membrane in order to establish the mechanism of electron transport [34–39]. Although all studies investigated the position of the *b* cytochromes, only the work of Glaser et al. [36] and Robertson and Dutton [37] on the cytochrome bc_1 complex of *R. capsulatus* directly measured the transfer of electrons between the uniquinone reduction site and cytochrome b_h (cytochrome *b*-560 in *R. capsula-*

Abbreviations: Hepes, *N*-2-hydroxyethylpiperazine-*N'*-2-ethanesulfonic acid; FCCP, carbonyl cyanide *p*-trifluoromethozyphenylhydrazone

Correspondence: T. Ohnishi, Department of Biochemistry and Biophysics, University of Pennsylvania, Philadelphia, PA 19104, USA.

tus). Both studies demonstrated that the electron transfer from cytochrome b_h to ubiquinone represented approx. 40–55% of the membrane dielectric. In addition, Robertson and Dutton concluded that the electrogenic change observed was the transfer of an electron towards the negative (N) side of the membrane, the side from which protons are taken up, rather than the translocation of a proton towards the positive (P) side. Both of these studies, however, are dependent on the assumption of the homogeneous dielectric constant of the protein. Unfortunately, the dielectric within the protein is not necessarily constant. Therefore, these studies could not unequivocally establish the position of the quinone reduction site within the membrane. In this paper we determine the distance of the semiquinone anion $Q_i^{\cdot-}$ from the surface of the cytochrome bc_1 complex by a method which is independent of the dielectric constant. We have used the enhancement of the spin relaxation of the EPR signal of $Q_i^{\cdot}$ by an external paramagnetic spin probe to determine this distance.

The membrane preparation used in these studies was carefully chosen. The cytochrome bc_1 complex of *R. capsulatus* is extremely simple, consisting of only three subunits (Ref. 40 and Robertson, D.E. personal communication) rather than the 8–12 found in the mitochondrial complex [1–3]. In this preparation, measurements of the position of $Q_i^{\cdot-}$ are not complicated by large noncatalytic subunits, represented by two core proteins [1–3]. Secondly, membrane particles, chromatophores, where the side from which protons are taken up is exposed (the side N) are easily obtained with at least 90% in the same membrane polarity. From this orientation the position of $Q_i^{\cdot-}$ should be easily estimated if it is near to the N side as proposed by most researchers. Lastly, our previous research has shown the possibility of spin relay through other paramagnetic species such as oxidized cytochromes [39]. Only at high pH values can the ubisemiquinone $Q_i^{\cdot-}$ be observed when the *b* cytochromes are reduced (diamagnetic). The cytochrome bc_1 complex of *R. capsulatus* is very tolerant of high pH values, up to pH 11, making it possible to perform these measurements with the *b* cytochromes reduced. In addition, we have used a strain of *R. capsulatus*, M2, which is deficient in both the succinate dehydrogenase and the NADH dehydrogenase activities [41] which removes many of the interfering background signals.

Materials and Methods

Chemicals

L-α-Phosphatidylcholine (egg) was obtained from Avante Polar Lipids (Birmingham, AL, USA). The spin-labeled fatty acid derivatives (C_5, C_7, C_{12} doxylstearic acid) were obtained from Molecular Probes, (Eugene, OR). Holmium nitrate was purchased from Alpha Products (Danvers, MA, USA). All other chemicals were obtained from Sigma Chemical Co. (St. Louis, MO, USA) or Aldrich Chemical Co. (Milwaukee, WI, USA) and were of the highest quality available.

EPR measurements

Cryogenic EPR spectroscopy and progressive microwave power saturation analyses were performed as previously described [42,43]. The curve fitting method defined by Blum and Ohnishi [43] as well as computer fitting [44] were used to calculate the half-saturation parameter, $P_{1/2}$. The spin relaxation enhancement effect by extrinsic paramagnetic probes, $\Delta P_{1/2}$ (mW/mmol), is expressed in terms of an effective distance (R), as in preceding papers [43,44]. The conversion of the value of $\Delta P_{1/2}$ to the effective distance (R) was performed using the following equation:

$$R_i(\text{Å}) = \left[(\Delta P_{1/2,\text{Std}} / \Delta P_{1/2,i})^{1/x} (R_{\text{Std}} + 5) \right] - 5 \qquad (1)$$

which was previously developed from experimental observations [42]. The exponential distance dependence term x has been experimentally determined to vary from 4 to 6 [39,42] and recently shown to vary theoretically from 3 to 6 depending on the type of preparation (membranous or soluble) and the shape of the protein [45]. We have used the $\Delta P_{1/2}$ determined in this work for 5-,7-,12-doxyl stearic acid as the standard in our calculations for the position of $Q_i^{\cdot-}$. The term $\Delta P_{1/2}$ is related to the spin–lattice relaxation time (T_1) and the spin–spin relaxation time (T_2) as shown by the Eqn. 2.

$$\Delta P_{1/2} \propto \frac{1}{T_1 T_2} \qquad (2)$$

Under our experimental conditions, $\Delta P_{1/2}$ is proportional to the spin probe concentration. For our samples, with varying concentrations of spin probes, T_2 is nearly constant in the temperature range used, therefore $\Delta P_{1/2}$ is proportional to the inverse of T_1 [43,44].

Sample preparation

Phospholipid vesicles were prepared as previously described [39,46] with the exception that the spin-labelled stearic acid derivative was added to the phospholipids at the beginning of the preparation. The n-doxylstearic acid, spin-labelled with the nitroxide radical on the C_5, C_7, or C_{12} position, was added in a ratio of 61 : 1 phospholipid to stearic acid. The distance from the head of the molecule of doxyl stearic acid incorporated into the vesicle to the spin label is well defined in each case. To aliquots of a preparation of phospholipid vesicles varying amounts of holmium (Ho^{3+}) complexed to EDTA were added and the sam-

ples were quickly frozen. For a control sample, diamagnetic lanthanum (La^{3+}) complexed to EDTA was added to the phospholipid vesicles.

Cells of *R. capsulatus* were grown as described in Ref. [47]. Chromatophores were made as described by Bowyer et al [48] with the exception that a cell pressure of 20000 lb/in^2 was used in the French Press. At the final stage of preparation the chromatophores were suspended in 50 mM Bistris-propane/100 mM KCl (pH 9.5). The following mediators were added; 60 μM of each of 2, 3, 5, 6-tetramethylparaphenylenediamine (DAD); 1,4-benzoquinone; 1,4-naphthoquinone; 1,2-naphthoquinone; and 2, 3, 5, 6-tetramethyl-1,4-benzoquinone (duroquinone). FCCP was added to a concentration of 0.83 μM. For each concentration of holmium-EDTA a 3-ml aliquot of the membrane particles were placed in an anaerobic redox vessel and poised at a redox potential (E_h) of 5–10 mV as described by Dutton [49]. Sequential samples of 0.3 ml were then taken with no addition, after the addition of either homium-EDTA or lanthanum-EDTA, and after the subsequent addition of antimycin (333 μM final concentration). Each sample was immediately frozen after being taken and stored in liquid nitrogen until used. The redox potential drifted less than 5 mV during the sampling time of the experiment.

Results

In order to ensure the highest accuracy in our measurements, we have developed a standard which closely approximates the properties of the system we intended to study. We have used the free radical formed by the nitroxide group of the doxyl spin label, which has been incorporated at known positions along the fatty acid hydrocarbon tail, as the model system for the organic free radical of the ubisemiquinone $Q_i^{\cdot-}$. Initially, the spin lattice relaxation time, T_1, of the spin labelled C_5, C_7, C_{10}, and C_{12} doxylstearic acid derivatives incorporated into one side of the membrane of phospholipid vesicles was measured through electron-spin echo spectroscopy [39]. In order to obtain reliable results, this measurement required relatively high concentrations of the component being measured. Because of this limitation the direct measurement of the spin-lattice relaxation time of $Q_i^{\cdot-}$ by the ESE method could not be made due to its low concentration within the chromatophore membrane. Therefore, we have extended our calibration to include progressive power saturation measurements by continuous-wave EPR spectroscopy.

In our present experiments, the spin-labelled stearic acid derivative was incorporated into both sides of the membrane. Since holmium, total angular momentum quantum number (J) of 7/2, is a relatively weak paramagnetic probe when compared to dysprosium (J = 15/2), only those spin labels on the outer half of the membrane would be affected. To account for this we have assumed that the stearic acid derivative will be arranged within the membrane in a fashion similar to the distribution of phospholipids. The phospholipid vesicles used in this study have a diameter of about 800 Å. For vesicles of this size and assuming a 40-Å thick membrane, the phospholipids are distributed 55% to 45%, outside the inside. To account for the fraction of spin labels not affected by the paramagnetic probe we

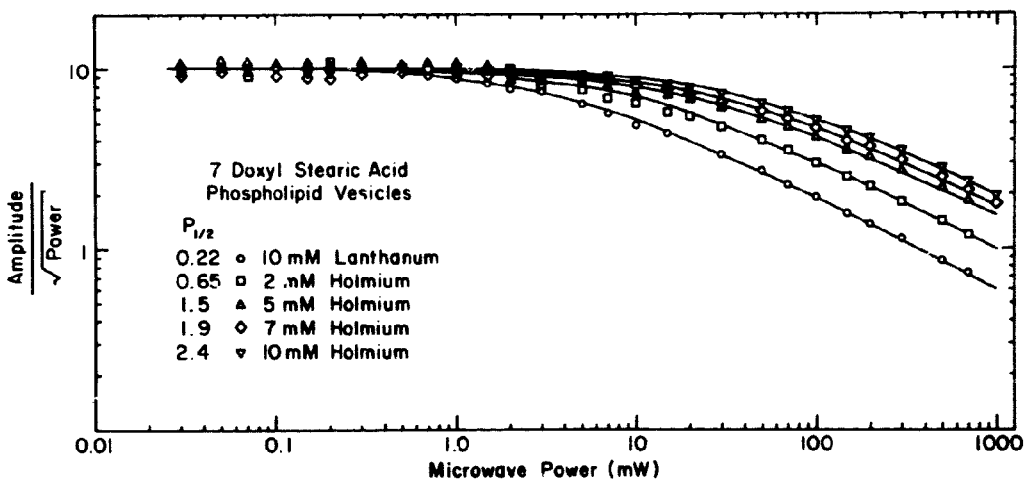

Fig. 1. Sequential power saturation of phospholipid vesicles containing C_7 doxylstearic acid with varying concentrations of holmium-EDTA. Phospholipid vesicles containing C_7 doxylstearic acid were suspended in 50 mM Hepes, 20 mM NaCl (pH 7.5). The EPR conditions were: Sweep width, 0.04 T; sweep rate, 0.01 Tesla/min; time constant, 0.064 s; modulation amplitude, $1 \cdot 10^{-4}$ T; microwave frequency, 9.316 GHz; sample temperature, 25 K.

have subtracted 45% of the signal amplitude observed in the absence of any paramagnetic probe from the signal observed in the presence of the paramagnetic probe at each of the microwave power settings. In Fig. 1 are plotted the data obtained from a progressive power saturation analysis of the C_7 doxystearic acid derivative incorporated into the phospholipid vesicles. As the concentration of the extrinsic spin probe, holmium-EDTA, was increased from 0 to 10 mM, the microwave power level at which the signal is half saturated, $P_{1/2}$, increased. At concentrations of 0, 2, 5, 7 and 10 mM holmium, $P_{1/2}$ values of 0.22, 0.65, 1.5, 1.9, and 2.4 mW, respectively, were obtained. Similar increases in the $P_{1/2}$ value were observed for each of the stearic acid derivatives studied.

Intrinsic relaxation of spin labels is very sensitive to its microenvironment. Thus, the $P_{1/2}$ value of each of the spin-labelled fatty acids, in the absence of an external paramagnetic probe, differed considerably, depending upon the position of the spin label on the hydrocarbon tail of the fatty acid. The $P_{1/2}$ values of 0.034, 0.22, and 0.30 mW were obtained for C_5, C_7, and C_{12} doxyl-stearic acid, respectively, revealing the faster spin relaxation (the higher freedom of the motion), the further away the spin label from the surface. A plot of the $P_{1/2}$ value versus the concentration of external paramagnetic probe resulted in a linear relationship for each spin-labelled fatty acid. The $\Delta P_{1/2}$ values (the slopes) obtained directly from the data were 0.06, 0.20, and 0.12 mW/mM holmium-EDTA for the C_5, C_7, and C_{12} doxylstearic acid, respectively. This analysis of the data leads to no apparent relationship between the distance of the spin labels from the surface and the individual $\Delta P_{1/2}$. This is due to the order of magnitude difference in the intrinsic spin relaxation rates among the C_5, C_7 and C_{12} derivatives. A more appropriate method of analyzing the data is to determine the effective change in the relaxation rate (expressed as $P_{1/2}$). It is accomplished by normalizing the data by the intrinsic relaxation rate of spin labels bound to different positions of the hydrocarbon tail. Plotted in Fig. 2 are the normalized $P_{1/2}$ values versus the concentration of external paramagnetic probe for each of the stearic acid derivatives, resulting in the linear relationship between the concentration of the external probe and the half-saturation power, $P_{1/2}$. Here, a plot of the $\Delta P_{1/2}$ versus distance shows a correlation with the best fit to an R^{-3} dependence (not shown). This result is in agreement with the theoretical treatment of Innes and Brudvig for this geometry [45]. Table I lists the $\Delta P_{1/2}$ values obtained from Fig. 2 as well as the distance of the spin labels from the surface.

Using these standard, we proceeded to measure the effect of various concentrations of holmium-EDTA on the normalized $P_{1/2}$ of the semiquinone anion, $Q_i^{\cdot-}$.

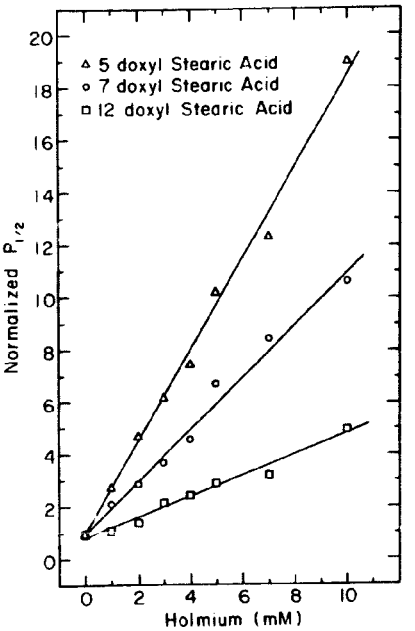

Fig. 2. Dependence of the normalized $P_{1/2}$ values of C_5, C_7, and C_{12} doxylstearic acid on the concentration of holmium-EDTA. Linear regression analysis of the data gives slopes of 1.76, 1.00, and 0.40 mM^{-1} holmium-EDTA, respectively, for C_5, C_7, and C_{12} doxylstearic acid. The values were normalized by dividing the $P_{1/2}$ values obtained at each concentration of holmium by the $P_{1/2}$ value obtained from the sample in the absence of holmium-EDTA.

Fig. 3 shows the EPR spectrum of the semiquinone signal observed in chromatophores obtained from *R. capsulatus* strain M2. This strain is deficient in both succinate dehydrogenase and NADH dehydrogenase activities [41]. At pH 9.5 in membrane particles of the wild-type strain, the antimycin insensitive signal represents approx. 45% of the total signal. As shown in Fig. 3, the antimycin-insensitive signal in strain M2 represents only about 30% of the signal. The spectrum of the antimycin-sensitive signal is typical of the $Q_i^{\cdot-}$ ubisemiquinone radical, ($g = 2.004$, $\Delta H = 0.84$ mT).

TABLE I

Summary of normalized $\Delta P_{1/2}$ dependence on holmium concentration

[1] R_{std} was calculated by assuming the carboxyl group would be located at the phosphate water interface of the phospholipids and calculating the linear distance to the doxyl group based on the angle of a single C–C bond of 109.5°.

Spin label	Normalized $\Delta P_{1/2}$ (1/mM holmium)	R^1_{std} (Å)
5-Doxylstearic acid	1.76	6.0
7-Doxylstearic acid	1.00	8.6
12-Doxylstearic acid	0.40	14.6

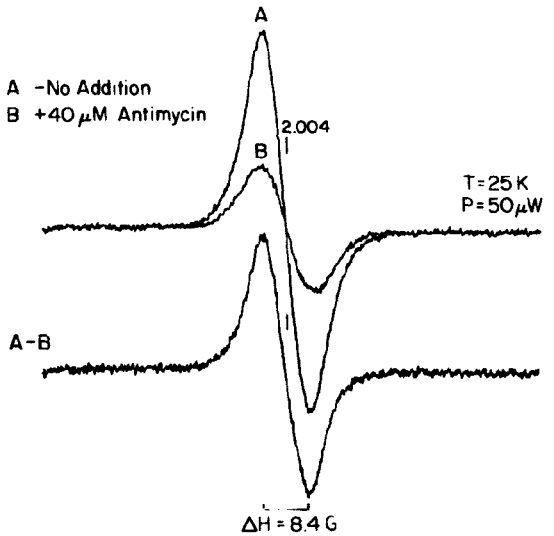

Fig. 3. EPR spectrum of Q_i^- in Chromatophores from *R. capsulatus* strain M2. Chromatophores of *R. capsulatus* strain M2 were suspended in 50 mM bistrispropane, 100 mM KCl (pH 9.5). The EPR conditions were: Gain, 2: 10^4; sweep width, 0.01 T; sweep rate, $2.5 \cdot 10^{-3}$ T/min; time constant, 0.128 s; modulation amplitude, $5 \cdot 10^{-4}$ T; microwave power, 0.05 mW; microwave frequency, 9.3176 GHz; sample temperature, 25 K.

The antimycin-insensitive signal also possesses a g value of 2.004 but has a spectral line width of 1.01 mT. Since the antimycin-insensitive semiquinone represented a significant portion of the signal, matched samples with and without antimycin were prepared at each holmium-EDTA concentration. The difference in the signal amplitudes was then plotted to give the power saturation curve. Fig. 4 gives examples of a few of the power saturation curves for the Q_i^- ubisemiquinone. If the homogeneity of the signal is allowed to vary during the fitting process the $P_{1/2}$ values obtained are 0.0105, 0.055, 0.092 and 0.180 mW for 0, 2, 4 and 8 mM holmium, respectively. The antimycin-sensitive signal obtained in this fashion appears to have been somewhat heterogeneous, since power saturation curves, which fit the data best, varied in the degree of homogeneity as the concentration of holmium was increased. The change in homogeneity may result from small changes in the spin-spin relaxation time, T_2, due to the added relaxant. Therefore, the power saturation curves were analyzed by two methods which should result in extreme cases for the distance measurement. One method was to allow the homogeneity to vary in the curve fitting process to obtain the $P_{1/2}$ value. The other method was to fix the homogeneity to a completely inhomogeneous line and record the $P_{1/2}$ value of the closest fit to the data. In Fig. 5 are plotted the $P_{1/2}$ values determined for the completely inhomogeneous curve (△) and for the best fit, allowing the homogeneity to vary (○). Through the data are drawn linear regression lines which give normalized $\Delta P_{1/2}$ values of 1.61 and 0.83 mM^{-1} holmium, respectively. Using Eqn. 1 and the $\Delta P_{1/2,std}$ and R_{std} values of the C-5 doxylstearic acid derivative (Table I) we obtain distances ranging from 6.6 to 9.5 Å, assuming an R^{-3} dependence. Table II provides the $P_{1/2}$ values obtained from the regression lines and the distances calculated from the surface of the protein to Q_i^- assuming an R^{-3} dependence and using each of the

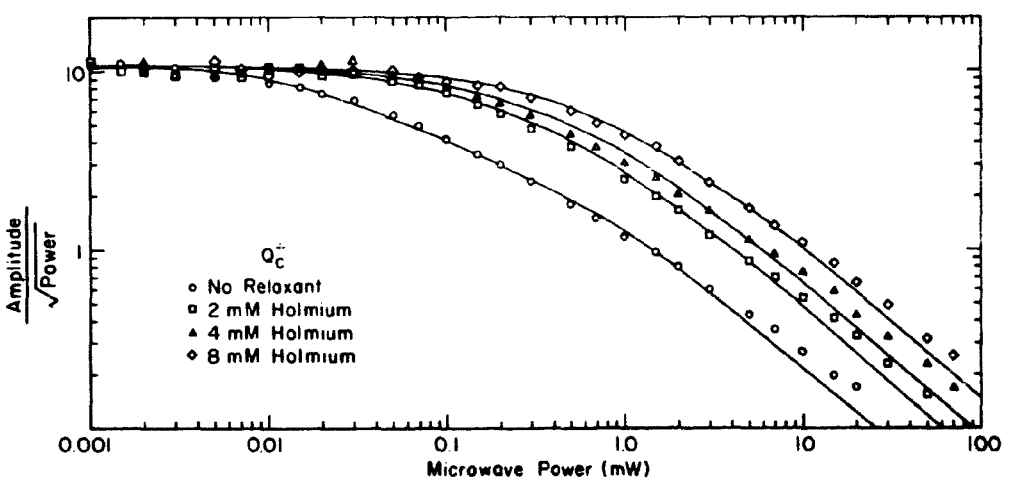

Fig. 4. Sequential power saturation of the ubisemiquinone Q_i^- in chromatophores of *R. capsulatus* strain M2. Chromatophores were suspended and redox poised as described in Materials and Methods. Holmium-EDTA was added at the concentration indicated. Plotted is the microwave power saturation profile of the difference between matched samples without minus with antimycin. The EPR conditions were: sweep width, 0.04 T; sweep rate, 0.01 T/min; time constant, 0.238 s; modulation amplitude, $5 \cdot 10^{-4}$ T; microwave frequency, 9.317 GHz; sample temperature, 25 K.

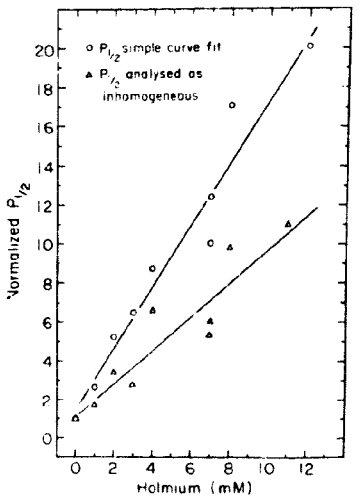

Fig. 5. Dependence of the normalized $P_{1/2}$ values of $Q_i^{\cdot-}$ on the concentration of holmium-EDTA. Power saturation curves of $Q_i^{\cdot-}$ at varying holmium-EDTA concentrations were analyzed as described in the text. Lines are derived from a linear regression analysis of the data and gave slopes of 1.61 and 0.83 mM^{-1} holmium-EDTA.

three standards. These data indicate that semiquinone anion $Q_i^{\cdot-}$ is between 6 and 10 Å from the protein surface on the N side.

As we discussed in the previous paper [39], this paramagnetic probe method is not a high-resolution technique. However, the distances of the $Q_i^{\cdot-}$ from the protein surface (presented in Table II) obtained using three different spin-label standards for each type of fit, covers a very narrow range. It indicates that the accuracy of the method and the standards used are very good. A rather large error range for the distance measurement of the $Q_i^{\cdot-}$ is considered to arise from the following reasons. (1) The $Q_i^{\cdot-}$ signals from the redox-poised chromatophore are intrinsically much weaker than the signals from the standard spin labels. (2) In addition to the possible heterogeneity of the signal, the Q_i species are measured as the antimycin-sensitive portion of the $g = 2.00$ transition. Thus, all data points recorded at different microwave power levels arise from the signal difference of the two EPR samples (± antimycin). Therefore, more scattered data points are expected. Nevertheless, the range of the values obtained amply demonstrates that the location of $Q_i^{\cdot-}$ is near the N side of the membrane and is neither the center of the membrane nor the other surface.

TABLE II

Distance of $Q_i^{\cdot-}$ from the protein surface

Standard	Type of fit	R^{-1} (Å)
5-Doxylstearic acid	simple curve fit	6.3
	inhomogeneous	9.1
7-Doxylstearic acid	simple curve fit	6.6
	inhomogeneous	9.5
12-Doxylstearic acid	simple curve fit	7.3
	inhomogeneous	10.4

Discussion

Our previous work on the bovine heart cytochrome bc_1 complex has shown that cytochrome *b*-566 and the Rieske iron–sulfur cluster are located near the level of the lipid/water interface on the P-side surface of the membrane and that cytochrome *b*-562 is located approximately in the center of the membrane [39]. Here we have extended our studies to the semiquinone anion radical, $Q_i^{\cdot-}$, which we have shown to be within 6–10 Å from the protein surface on the N side of the membrane. Interpretation of our previous results on the bovine complex was aided by the availability of a low resolution three dimensional structural model of the ubiquinonol–cytochrome *c* oxidoreductase in *Neurospora crassa* mitochondria. This model was obtained by reconstitution of three-dimensional images obtained by tilted electron microscopic views of two-dimensional membrane crystals of the *N crassa* cytochrome bc_1 complex [50]. Although we do not have similar information for the *R. capsulatus*, it is a much simpler system consisting of only three subunits, the cytochromes *b* and c_1 and the Rieske iron–sulfur protein. In this system the portion of the complex which extends out of the membrane on the $Q_i^{\cdot-}$ side of the complex is composed only of the cytochrome *b* subunit. Calculations based on the amino-acid sequence [40], the number of helices within the complex [51,52], the volume of the amino acids [53], and the possible shapes for the complex have led to the following conclusion. If $Q_i^{\cdot-}$ is near the lipid/protein interface, it will be at most 10 Å from the surface of the lipid bilayer, assuming that there are no large indentations into the complex. If $Q_i^{\cdot-}$ is buried within the protein complex, it will be much nearer to the lipid surface level and may extend out of the lipid bilayer, depending on the size and shape of the portion of cytochrome *b* which protrudes out from the cytoplasmic membrane. This view is exemplified by the drawing in Fig. 6. Recently, Salerno et al. [54] have reported that $Q_i^{\cdot-}$ is approx. 6 Å from the exchangeable protons within the mitochondrial cytochrome bc_1 complex. In the mitochondrial complex the large portion of the protein which protrudes on the N side of the membrane (Fig. 6) has been suggested to be composed mostly of core proteins I and II, largest subunits of cytochrome bc_1. The results of Salerno et al. [54] indicate that $Q_i^{\cdot-}$ is near to the edge of the complex or that there exists a significant proton well to allow the exchange of protons with $Q_i^{\cdot-}$. If we

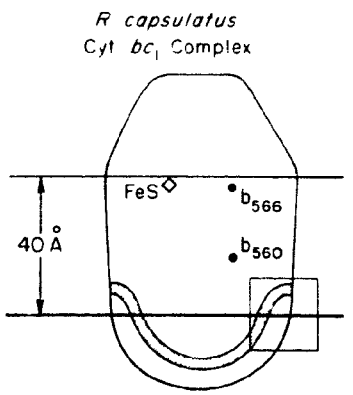

Fig. 6. Models of the *R. capsulatus* Cytochrome bc_1 complex. Represented in the figure is the cytochrome bc_1 complex of *R. capsulatus*. The hatched area represents the possible locations of $Q_i^{\cdot-}$ within the complex. The boxed region represents the area we consider most likely for the position of $Q_i^{\cdot-}$.

combine these results with our observations, it is likely that $Q_i^{\cdot-}$ is located near the corner of the protein/lipid/aqueous interface (shown as boxed in Fig. 6) and is close to the surface level of the lipid bilayer.

The model presented in Fig. 6 is consistent with the carotenoid band-shift data of Robertson and Dutton [37] and Glaser et al. [36] in which they find that the distance from cytochrome *b*-561 to $Q_i^{\cdot-}$ represents half of the dielectric and that the distance from cytochrome *b*-566 to cytochrome *b*-561 represents the other half of the dielectric. These data are also in agreement with the conclusion that the antimycin binding site is 17 Å from cytochrome *b*-562 if we conclude that the portion of antimycin which fluoresces is bound at the $Q_i^{\cdot-}$ binding site [55].

Although EPR and fluorescence data are consistent with that of the carotenoid band shift, there is one group of observations which are not easly explainable. EPR redox titrations on the isolated yeast cytochrome bc_1 complex [56,57] and the bovine heart complex [58] have indicated that there is spin coupling between a quinone moiety and cytochrome *b*-561^{+3}. Optical redox titrations of Rich et al. [11] have also suggested that there is a close association of a quinone species and cytochrome *b*-561. The thermodynamic properties of this quinone species did not follow those of the $Q_i^{\cdot-}$. It has been suggested that there is possibly an additional quinone molecule within the complex which is not EPR detectable [11,57]. Unless one assumes long-range interactions between $Q_i^{\cdot-}$ and cytochrome *b*-562, the suggestion of an additional quinone moiety is the only explanation which is consistent with our present and previous results and those discussed above. Resolution of the discrepancy between our results and the above observations will have to wait for further studies.

Acknowledgements

We would like to thank Dr. B.L. Marrs for providing us *R. capsulatus* M2 mutant strain. We would also like to thank Dawn Gangi for her technical assistance. This work was partially supported by NIH GM30736 and NSF DMB88-19305 to (T.O.) and NSF EPSCoR Grant RII-8610675 to the State of North Dakota (S.M.).

References

1 Hatefi, Y. (1978) Methods Enzymol. 53, 35–40.
2 Schägger, H. Link, T.A., Engle, W.D. and Von Jagow, G. (1986) Methods Enzymol. 126, 224–237.
3 Ljungdahl, P.O., Pennoye, J.D. and Trumpower, B.L. (1986) Methods Enzymol. 126, 181–191.
4 Rieske, J.S., Hansen, R.E. and Zaugg, W.S. (1964) J. Biol. Chem. 239, 3017–3022.
5 Trumpower, B.L. and Katki, A.G. (1979) in Membrane proteins in energy transduction (Capaldi, R.A. ed.), pp. 89–200, Academic Press, New York.
6 Wikström, Krab, K. and Saraste, M. (1981) Annu. Rev. Biochem. 50: 623–655.
7 Slater, E.C. (1973) Biochim. Biophys. Acta 301, 129–154.
8 von Jagow, G. and Link, T.A. (1986) Methods Enzymol. 126, 253–271.
9 Trumpower B.L. (1981) Biochim. Biophys. Acta 639, 129–155.
10 Berden, J.A. and Overdoes, F.R. (1972) Biochim Biophys. Acta 267, 7–14.
11 Rich, P.R., Jeal, A.E., Madgwick, S.A. and Moody, A.J. (1990) Biochim. Biophys. Acta 1018, 29–40.
12 Crofts, A.R. and Wraight, C.A. (1983) Biochim. Biophys. Acta 726, 149–185.
13 Dutton, P.L. (1968) in Encylcopedia of plant physiology (Staehelin, A. and Arntzen, C.J., eds.), Vol. 19, pp. 197–237, Springer, Berlin.
14 Mitchell, P. (1976) J. Theor. Biol. 62, 327–367.
15 Crofts, A.R., Meinhardt, S.W., Jones, K.R. and Snozzi, M. (1983) Biochim. Biophys. Acta 723, 202–218.
16 Trumpower, B.L. (1990) J. Biol. Chem. 265, 11409–11412.
17 Thierback, G. and Reichenback, H. (1981) Biochim. Biophys. Acta 638, 282–289.
18 Meinhardt, S.W. and Crofts, A.R. (1982) FEBS Lett. 149, 217–222.
19 von Jadow, G., Ljungdahl, P.O., Graff, P. Ohnishi, T. and Trumpower, B.L. (1984) J. Biol. Chem. 259, 6318–6326.
20 Bowyer, J.R., Dutton, P.L., Prince, R.C. and Crofts, A.R. (1980) Biochim. Biophys. Acta 592, 445–460.
21 Bowyer, J.R., Edwards, C.A., Ohnishi, T. and Trumpower, B.L. (1982) J. Biol. Chem. 257, 8321–8330.
22 Thierback, G., Kunze, B., Reichenback, H. and Hofle, G. (1984) Biochim. Biophys. Acta 765, 227–235.
23 Von Jagow, G. and Ohnishi, T. (1985) FEBS Lett. 185, 311–315.
24 DeVries, S., Albracht, S.P.J., Berden, J.A. and Slater, E.C. (1982) J. Biol. Chem. 256, 1196–1198.
25 Konstanchinov, A.A. and Ruuge, E.K. (1977) FEBS Lett. 81, 137–141.
26 Yu, C.-A., Nagaoka, S., Yu, L. and King, T.E. (1978) Biochem. Biophys. Res. Commun. 82, 1070–1078.
27 Ohnishi, T. and Trumpower, B.L. (1980) J. Biol. Chem. 255 3278–3284.
28 Salerno, J.C. and Ohnishi, T. (1980) Biochem. J. 192, 769–781.
29 De Vries, S., Berden, J.A. and Slater, E.C. (1980) FEBS Lett. 122, 143–148.

30 Meinhardt, S.W., Yang, X., Trumpower, B.L. and Ohnishi, T. (1987) J. Biol. Chem. 262, 8702–8706.
31 Robertson, D.E., Prince, R.C., Bowyer, J.R., Matsuura, K., Dutton, P.L. and Ohnishi, T. (1984) J. Biol. Chem. 259, 1758–1763.
32 Andrews, K.M., Crofts, A.R. and Gennis, R.B. (1990) Biochem. 29, 2645–2651.
33 Yu, L., Mei, Q.C. and Yu, C.A. (1984) J. Biol. Chem. 259, 5732–5760.
34 Konstantinov, A., Kunz, W.S. and Kamensky, Y.A. (1981) in Chemiosmotic Proton Circuits in Biological Membranes (Skulachev, V.P., and Hinkle, P.L., eds.), pp. 123–146, Addison-Wesley, Reading, MA.
35 Gopher, A. and Gutman, M. (1982) in Function of Quinones in Energy Conserving Systems, (Trumpower, B.L., ed.), pp. 511–526, Academic Press, New York.
36 Glaser, E.G. and Crofts, A.R. (1984) Biochim. Biophys. Acta 766, 322–333.
37 Robertson, D.E. and Dutton, P.L. (1988) Biochim. Biophys. Acta 935, 273–291.
38 Konstantinov, A. and Popova, E. (1987) in Cytochrome Systems, Molecular Biology and Bioenergetics (Papa, S., Chance, B.L. and Ernster, L., eds.), pp. 751–765, Plenum Press, New York.
39 Ohnishi, T., Schagger, H., Meinhardt, S.W., LoBrutto, R., Link, T.A. and Von Jagow, G. (1989) J. Biol. Chem. 264, 735–744.
40 Davidson, E. and Daldal, F. (1987) J. Mol. Biol. 195, 13–24.
41 Marrs, B. and Guest, H. (1973) J. Bacteriol. 114, 1045–1051.
42 Blum, H., Bowyer, J.R., Cusanovich, M.A., Waring, A.J. and Ohnishi, T. (1983) Biochim. Biophys. Acta 748, 418–428.
43 Blum, H. and Ohnishi, T. (1980) Biochim. Biophys. Acta 621, 9–18.
44 Blum, H., Cusanovich, M.A., Sweeney, W.V. and Ohnishi, T. (1981) J. Biol. Chem. 256, 2199–2206.
45 Innes, J.B. and Brudvig, G.W. (1989) Biochemistry 28, 1116–1125.
46 Enoch, H.G. and Strittmatter, P. (1979), Biochemistry 76, 145–149.
47 Dutton, P.L., Petty, K.M., Bonner, H.S. and Morse, S.P. (1975) Biochim. Biophys. Acta 387, 536–556.
48 Bowyer, J.R., Tierney, G.V. and Crofts, A.R. (1979) FEBS Lett. 101, 201–206.
49 Dutton, P.L. (1978) Methods Enzymol. 54, 411–435.
50 Karlsson, B. Hovmöller, S., Weiss, H. and Leonard, K. (1983) J. Mol. Biol. 165, 287–302.
51 Crofts, A.R., Robinson, H., Andrews, K.M., van Doren, S. and Berry, E. (1987) in Cytochrome Systems: Molecular Biology and Bioenergetics (Papa, S., Chance, B. and Ernster, L., eds.), pp. 617–624, Plenum, New York.
52 Brasseur, R. (1988) J. Biol. Chem. 263, 12571–12575.
53 Zamyatnin, A.A. (1972) Prog. Biophys. Mol. Biol. 24, 109–123.
54 Salerno, J.C., Osgood, M., Liu, Y., Taylor, H. and Scholes, C.P. (1990) Biochemistry 29, 6987–6993.
55 Berden, J.A. and Slater, E.C. (1972) Biochim. Biophys. Acta 256, 199–215.
56 Siedow, J.N., Power, S., De la Rosa, F.F. and Palmer, G. (1978) J. Biol. Chem. 253, 2392–2399.
57 De la Rosa, F.F. and Palmer, G. (1983) FEBS Lett. 163, 140–143.
58 Salerno, J.C., Xu, Y., Osgood, M.P., Kim, C.H. and King, T.E. (1989) J. Biol. Chem. 264, 15398–15403.